The Astrophysical Journal Letters, 714:L181–L184, 2010 May 10 doi:10.1088/2041-8205/714/2/L181

LUMINOUS X-RAY ACTIVE GALACTIC NUCLEI IN CLUSTERS OF GALAXIES

E. Koulouridis[1] and M. Plionis[1,2]
[1] Institute of Astronomy & Astrophysics, National Observatory of Athens, I. Metaxa & B. Pavlou, P. Penteli 152 36, Athens, Greece; ekoulour@astro.noa.gr
[2] Instituto Nacional de Astrofísica Óptica y Electrónica, 72840 Puebla, Pue, Mexico
Received 2009 December 8; accepted 2010 March 3; published 2010 April 12

ABSTRACT

We present a study of X-ray active galactic nucleus (AGN) overdensities in 16 Abell clusters, within the redshift range $0.073 < z < 0.279$, in order to investigate the effect of the hot inter-cluster environment on the triggering of the AGN phenomenon. The X-ray AGN overdensities, with respect to the field expectations, were estimated for sources with $L_x \geqslant 10^{42}$ erg s^{-1} (at the redshift of the clusters) and within an area of 1 h_{72}^{-1} Mpc radius (excluding the core). To investigate the presence or absence of a true enhancement of luminous X-ray AGNs in the cluster area, we also derived the corresponding optical galaxy overdensities, using a suitable range of *r*-band magnitudes. We always find the latter to be significantly higher (and only in two cases roughly equal) with respect to the corresponding X-ray overdensities. Over the whole cluster sample, the mean X-ray point-source overdensity is a factor of ∼4 less than that corresponding to bright optical galaxies, a difference which is significant at a >0.995 level, as indicated by an appropriate student's *t*-test. We conclude that the triggering of luminous X-ray AGNs in rich clusters is strongly suppressed. Furthermore, searching for optical Sloan Digital Sky Survey counterparts of all the X-ray sources, associated with our clusters, we found that about half appear to be background QSOs, while others are background and foreground AGNs or stars. The true overdensity of X-ray point sources, associated with the clusters, is therefore even smaller than what our statistical approach revealed.

Key words: galaxies: active – galaxies: clusters: general – X-rays: galaxies – X-rays: galaxies: clusters – X-rays: general

Online-only material: color figures

1. INTRODUCTION

There is a growing body of studies investigating the effect of the environment on the nuclear activity of galaxies and on the possible triggering mechanisms of the active galactic nucleus (AGN) phenomenon (e.g., Dultzin-Hacyan et al. 1999; Koulouridis et al. 2006, 2009; Sorrentino et al. 2006; González et al. 2008; Choi et al. 2009; Silverman et al. 2009; Lee et al. 2010; von der Linden et al. 2009; Padilla et al. 2009; and references therein).

One particular research direction is the study of X-ray AGNs, as a function of environment, since undoubtedly, one of the best AGN identification methods is through X-ray observations. Clusters of galaxies offer an ideal target for this type of study and indeed most X-ray based studies report overdensities of X-ray sources in clusters, with respect to the field (e.g., Cappi et al. 2001; Molnar et al. 2002; D'Elia et al. 2004; Branchesi, et al. 2007; Galametz et al. 2009; Gilmour et al. 2009).

There are attempts to substantiate such results with spectroscopic data and indeed various studies have verified the existence of a large population of X-ray AGNs in clusters of galaxies and its probable evolution with redshift (e.g., Martini et al. 2002, 2007, 2009; Johnson et al. 2003; van Breukelen et al. 2009). Some of the previous studies have also shown that only a small fraction of the X-ray sources, associated with clusters of galaxies, possess optical emission line ratios characteristic of AGN (also see Davis et al. 2003, Finoguenov et al. 2004). Similarly, starting from optical spectroscopy, Arnold et al. (2009) found that 14 out of 144 galaxy members of 11 clusters and groups are AGNs, but with only one being detected in X-rays. A similar trend of disconnection between X-ray and optically selected AGN, in eight poor groups of galaxies, was also found by Shen et al. (2007).

We believe that there is a major question still not adequately answered, which is: Is there an enhancement of AGN activity and/or of its X-ray manifestation in clusters of galaxies with respect to what expected from the obvious optical galaxy overdensity? We attempt to address this question by searching not only for the presence of a cluster X-ray AGN excess with respect to the field, since such could be expected on the basis of the known excess of optical galaxies in clusters, but rather by investigating whether the X-ray AGN overdensity shows a relative enhancement or suppression with respect to the corresponding optical galaxy overdensity.

2. SAMPLE SELECTION AND METHODOLOGY

The clusters of galaxies used in this study were selected according to the following criteria. (1) They belong to the list of Abell clusters (Abell et al. 1989), to ensure a relatively large number of member galaxies. (2) They have been observed by *XMM-Newton* with an exposure time, in each of the three detectors, of more than 10 ks. This is to ensure adequate photon-counts and to reach a relatively low flux limit. (3) The diffuse X-ray emission of the cluster, in the center of the field, is not as strong as to make impossible the detection of point sources located more than 0.5 h_{72}^{-1} Mpc from the center, at worst. (4) They lie in the area covered by the Sloan Digital Sky Survey (SDSS), in order to facilitate the search of optical counterparts of the X-ray point sources.

When this study began in 2006, 16 galaxy clusters with redshift $0.073 \leqslant z \leqslant 0.279$ were found to meet the above conditions. Our main aim was to calculate the density of X-ray sources in the clusters region and compare it with the corresponding density of optical galaxies. The cluster list, their

Table 1
Our Cluster Sample: X-ray and Optical Galaxy Overdensities and X-ray Source Categorization

Cluster	z	δ_x	$L_x^{\rm limit}$ (erg s^{-1})	N_x	$N_{\rm QSO}$	$N_{\rm cgal}$	$N_{\rm other}$	δ_o	N_g[a]
A2065	0.073	$2.00^{+1.80}_{-1.20}$	1.0e42	6	4	1	1	12.79 ± 3.37[b]	109
A1589	0.073	$2.96^{+1.96}_{-1.38}$	1.0e42	8	5	···	3	4.75 ± 2.22	38
A2670	0.076	$1.00^{+1.59}_{-0.97}$	1.0e42	4	1	···	3	6.26 ± 2.36	142
A1663	0.084	$3.08^{+1.75}_{-1.27}$	1.0e42	10	5	···	5	4.72 ± 2.01	56
A1750	0.085	$1.23^{+1.20}_{-0.68}$	1.0e42	3	2	···	1	4.58 ± 1.92	40
A1674	0.107	$2.41^{+1.37}_{-1.02}$	1.0e42	11	5	1	5	2.61 ± 1.43	165
A2050	0.118	$1.32^{+1.06}_{-0.76}$	1.0e42	9	2	···	7	2.19 ± 1.17	50
A1068	0.138	$0.31^{+0.65}_{-0.46}$	1.0e42	8	5	1	2	2.27 ± 1.11	71
A1689	0.183	$-0.18^{+0.65}_{-0.40}$	1.0e42	4	2	1	1	4.51 ± 1.14	228
A963	0.206	$0.05^{+0.83}_{-0.51}$	1.5e42	4	1	···	3	3.18 ± 0.90	134
A773	0.217	$0.25^{+0.99}_{-0.61}$	1.8e42	4	2	···	2	3.47 ± 0.88	108
A1763	0.223	$-0.05^{+1.26}_{-0.63}$	2.5e42	2	1	1	···	3.35 ± 0.86	152
A267	0.230	$0.32^{+1.05}_{-0.64}$	2.1e42	4	1	···	3	2.18 ± 0.69	37
A1835	0.253	$0.03^{+1.37}_{-0.68}$	3.5e42	2	1	1	···	2.61 ± 0.67	48
A2631	0.273	$1.19^{+1.49}_{-0.95}$	3.3e42	5	4	···	1	1.55 ± 0.52	136
A1758	0.279	$0.61^{+1.28}_{-0.78}$	2.2e42	4	3	···	1	3.42 ± 0.69	198

Notes.
[a] N_g is the Abell richness, from Abell et al. (1989).
[b] Using the local background estimate, we obtain $\delta_o \simeq 4.9 \pm 1.4$.

redshift, and various characteristics, determined in the present study, are shown in Table 1.

The corresponding 16 *XMM* cluster fields were analyzed using the Science Analysis Software (SAS) of the *XMM-Newton*. For the final extraction of sources, we merged the images from all three detectors (MOS1, MOS2, and pn) in the energy range 0.5–8 keV (at the observers frame) and selected the sources located within a radius of 1 h_{72}^{-1} Mpc from the center of the cluster and 5σ above the background. We then extracted the flux of the detected sources, its corresponding X-ray luminosity at the redshift of the cluster assuming a power-law spectrum with $\Gamma = 1.7$ and the sensitivity of the detectors in each pixel of our fields. Since the sensitivity varies greatly across the field of view, mostly due to vignetting, we constructed the sensitivity map for each *XMM* field in order to eventually calculate accurately the theoretically expected number of sources in each region of interest.

Due to the fact that the diffuse cluster X-ray emission can be strong enough to hide point sources, we have excluded from our analysis the central region of each cluster. This was determined by adjusting a King's profile (King 1962) to the diffuse emission, and deriving the cluster core radius, which is different for each cluster and ranges from ∼20 to 170 h_{72}^{-1} kpc. In order to efficiently remove the influence of the diffuse emission of the central cluster area, we consistently used for all clusters an inner radial cutoff of $3\times r_c$. We however remind the reader that there are indications, from *Chandra* data, of an increasing AGN population toward the centers of clusters (e.g., Ruderman & Ebeling 2005; Martini et al. 2007; Gilmour et al. 2009), which we cannot, however, efficiently probe with *XMM-Newton*.

We then counted all X-ray sources with luminosity $L_x \geqslant 10^{42}$ erg s^{-1} (N_x) located within the effective cluster region (i.e., the annulus between $3 \times r_c$ and 1 h_{72}^{-1} Mpc). The corresponding expected number of X-ray AGNs (N_e) was estimated by using the $\log N - \log S$ of Kim et al. (2007) folding in the sensitivity map of each field. The overdensity of X-ray sources in each cluster was then calculated according to $1+\delta_x = N_x/N_e$, and its uncertainty by using the small number Poisson approximation (e.g., Gehrels 1986) for a confidence level corresponding to the 1σ limit for Gaussian statistics (i.e., 0.8413). The robustness of the derived values of δ_x to uncertainties (1) of the $\log N - \log S$ relation and (2) of the overdensity determination method was verified by varying the $\log N - \log S$ relation within its quoted uncertainties and by alternatively using the overdensity estimation method of Branchesi et al. (2007, their Equation (6)). No significant variations of δ_x and of its uncertainty were found.

To calculate the corresponding overdensity of SDSS optical galaxies, and to minimize as much as possible projection effects, we extracted all galaxies located within 5 h_{72}^{-1} Mpc around the cluster center (to also facilitate the estimate of the local background), having magnitudes in the range $m_r^* - 0.5 < m_r < m_r^* + 0.5$, where m_r^* is the r-band magnitude corresponding to M_r^* of the Blanton et al. (2003) luminosity function at the redshift of the cluster. This characteristic magnitude, corresponding to the break of the luminosity function, is estimated by $m^* = M^* + 5\log_{10} d_L + K(z) + 25 + A_\nu$, with d_L the luminosity distance of the cluster (for the "concordance" cosmology), $K(z)$ the K-correction for an elliptical galaxy spectral energy distribution (based on Poggianti 1997), and A_ν the Galactic absorption, calculated using Galactic absorption maps of Schlegel et al. (1998). We then counted the corresponding optical galaxies in the effective cluster area and compared with a global and/or a local background estimate, consistently for the corresponding magnitude range of each cluster. The former was determined from a 20 deg^2 region near the equatorial coordinate equator, while the latter from the annulus between 4 and 5 h_{72}^{-1} Mpc around each cluster center, a distance far enough to ensure negligible contamination by cluster galaxies. The overdensity results are robust to the different background estimates, with the only exception of A2065, which appears to be embedded in an overall high large-scale overdensity. We choose to present optical overdensity results based on the global background estimate.

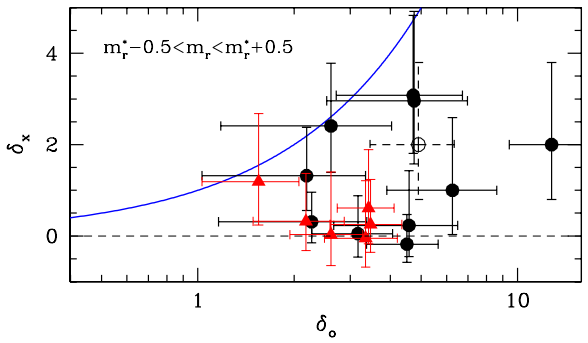

Figure 1. X-ray AGN overdensity δ_x with respect to overdensity of SDSS bright galaxies, δ_o. Triangles denote the clusters with flux limit corresponding to $L_x \gtrsim 2 \times 10^{42}$ erg s^{-1} (all $z \gtrsim 0.2$ clusters; see Table 1), while filled circles denote lower-z clusters with $L_x \simeq 10^{42}$ erg s^{-1}. The empty dot corresponds to A2065 when using its local background. The continuous curve corresponds to $\delta_x = \delta_o$, while the dashed line to $\delta_x = 0$. The errorbars correspond to Poisson uncertainties.

(A color version of this figure is available in the online journal.)

Finally, the overdensity of optical galaxies in clusters was calculated in the usual way, i.e., $1 + \delta_o = N_o/\langle N \rangle$, with corresponding Poisson uncertainty of $\sigma^2_{\delta_o} \simeq \Delta_o[1+\sigma_b^2\Delta_o]$, where $\Delta_o = (1 + \delta_o)^2/N_o$ and σ_b is the Poisson uncertainty of the background optical galaxy density, with a typical value being $\sim$0.025.

3. RESULTS AND CONCLUSIONS

We find that there is a relatively significant X-ray source overdensity in about half of the clusters in our sample, the rest showing the excepted background value of δ_x. This can be realized by inspecting Table 1, where we list the X-ray and optical overdensity values and their uncertainties, as well as from Figure 1 where we plot the cluster X-ray point-source overdensities versus the corresponding optical SDSS galaxy overdensities, within the indicated r-band magnitude range. Note that the six clusters with effective X-ray flux limit corresponding to a minimum luminosity of $L_x \gtrsim 2 \times 10^{42}$ erg s^{-1} (see specific values in Table 1), at the redshift of the clusters, are indicated by a triangular point type.

Although the number of clusters in our sample is quite low to provide stringent population statistics, a secure and important conclusion of our analysis is that the cluster X-ray point-source overdensities are always lower than the corresponding optical SDSS overdensities (with only two clusters having $\delta_x \sim \delta_o$). In Table 2, we present such population statistics but separately for the two cluster subsamples having different limiting L_x (as discussed previously). Also note that in order to take into account the variable uncertainty of the overdensity values, we present in Table 2 the Poisson uncertainty-weighted mean optical and X-ray overdensities. A student's t-test comparing the two means, assuming unknown and unequal variances, shows that they are different at a high significance level (see

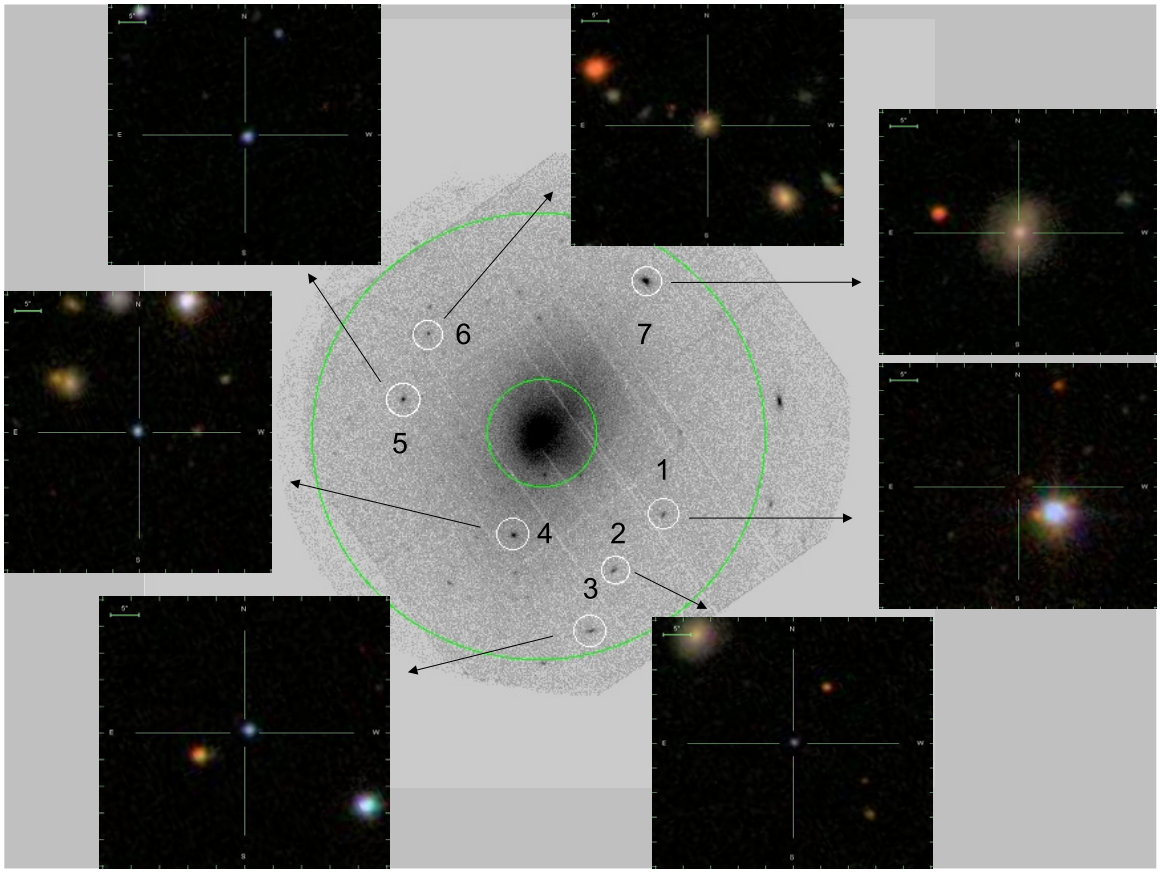

Figure 2. Example of the X-ray image of a cluster field from our sample (Abell 2065). The green circles delineate the inner and outer radii, within which we measure overdensities. The SDSS gri-composite image possibly corresponds to a star. Images 2, 3, 4, and 5 are probable background QSO, image 6 corresponds to a cluster galaxy (as indicated by its photometric redshift) but with $L_x < 10^{42}$ erg s^{-1} (and thus not included in our analysis), while image 7 corresponds to a $L_x \geqslant 10^{42}$ erg s^{-1} Seyfert 1 belonging to the cluster ($z = 0.0747$).

(A color version of this figure is available in the online journal.)

Table 2
Population Statistics for Our Cluster Sample

$L_x^{\rm limit}$ (erg s^{-1})	No.	$\langle\delta_x/\delta_o\rangle$	$\langle\delta_x\rangle_w$ [a]	$\langle\delta_o\rangle_w$ [a]	$1-\mathcal{P}$ [b]
1×10^{42}	10	0.33 ± 0.34	0.91 ± 0.76	3.99 ± 1.89	0.995
$\gtrsim 2\times10^{42}$	6	0.19 ± 0.29	0.36 ± 0.34	2.65 ± 1.10	0.999

Notes.
[a] $\langle\delta_x\rangle_w$ and $\langle\delta_o\rangle_w$ correspond to Poisson uncertainty-weighted means.
[b] $\mathcal{P}$ is the probability that the unweighted $\langle\delta_o\rangle$ and $\langle\delta_x\rangle$ are equal. The corresponding probability for the weighted means is even larger.

$\mathcal{P}$ in Table 2). Inspecting Table 2, it becomes evident that the luminous X-ray AGN overdensity is suppressed by a factor of 3–4, on the mean, with what would have been expected from a constant fraction, independent of environment, of X-ray AGNs to bright optical galaxies. This result is in the same direction with the optical SDSS analysis of Lee et al. (2010).

In order to investigate in more detail the nature of the X-ray overdensities in our cluster sample, we have also cross-identified all detected X-ray sources with the SDSS database, finding in total only six out of the 88 detected X-ray point sources (with $L_x \geqslant 10^{42}$ erg s^{-1} at the redshift of the cluster) being clearly associated with the clusters; among which one spectroscopically confirmed AGN (Sy1), two galaxies with no apparent emission lines, and three more galaxies, based on their photometric redshifts (one of which, in A1689, is indeed confirmed by the spectroscopic analysis of Martini et al. 2007). In Table 1, we also present the optical characterization of the X-ray point sources, the total number of which for each cluster field, N_x, is listed in Column 5. The sixth column indicates the number of probable background QSO, $N_{\rm QSO}$, (mostly determined as such from their point-like images and their $u-g$ versus $g-r$ colors, while $\sim$10% are also spectroscopically verified), the seventh column indicates the number of X-ray sources clearly associated with cluster galaxies, $N_{\rm cgal}$, and the eighth column indicates the number of apparently irrelevant associations, $N_{\rm other}$, like stars, foreground/background galaxies, no-counterparts, smudges, etc. About $\sim$50% of all our AGN candidates appear to be related to background QSO, which in many clusters represent the expected background provided by the $\log N - \log S$ of Kim et al. (2007). Therefore, the real overdensity of X-ray AGNs associated with our cluster sample appears to be significantly smaller than what is listed in Column 3 of Table 1, a fact which further strengthens our main result that the rich cluster environment (within 1 h_{72}^{-1} Mpc) strongly suppresses the luminous X-ray AGN activity.

In order to also provide a visual example of the source categorization, we present in Figure 2 the *XMM* field of A2065, the lowest z cluster of our sample, together with the SDSS composite gri-band images of all the X-ray point-source counterparts.

Finally, we stress that the main conclusion of our present analysis is that in the intermediate intracluster distances (i.e., between $3r_c$ and 1 h_{72}^{-1} Mpc), the relatively dense and hot ICM environment not only does not enhance AGN activity, but also rather strongly suppresses it (at least its X-ray luminous manifestation).

We thank I. Georgantopoulos for discussions and the referee for useful suggestions. M. Plionis acknowledges financial support under Mexican government CONACyT grant 2005-49878. Funding for the SDSS and SDSS-II has been provided by the Alfred P. Sloan Foundation, the Participating Institutions, the National Science Foundation, the U.S. Department of Energy, the National Aeronautics and Space Administration, the Japanese Monbukagakusho, the Max Planck Society, and the Higher Education Funding Council for England. The SDSS Web site is http://www.sdss.org/.

REFERENCES

Abell, G. O., Corwin, H. G., Jr., & Olowin, R. P. 1989, ApJS, 70, 1
Arnold, T. J., Martini, P., Mulchaey, J. S., Berti, A., & Jeltema, T. E. 2009, ApJ, 707, 1691
Blanton, M. R., et al. 2003, ApJ, 592, 819
Branchesi, M., Gioia, I. M., Fanti, C., Fanti, R., & Cappelluti, N. 2007, A&A, 462, 449
Cappi, M., et al. 2001, ApJ, 548, 624
Choi, Y.-Y., Woo, J.-H., & Park, C. 2009, ApJ, 699, 1679
Davis, D. S., Miller, N. A., & Mushotzky, R. F. 2003, ApJ, 597, 202
D'Elia, V., Fiore, F., Elvis, M., Cappi, M., Mathur, S., Mazzotta, P., Falco, E., & Cocchia, F. 2004, A&A, 422, 11
Dultzin-Hacyan, D., Krongold, Y., Fuentes-Guridi, I., & Marziani, P. 1999, ApJ, 513, L111
Finoguenov, A., Briel, U. G., Henry, J. P., Gavazzi, G., Iglesias-Paramo, J., & Boselli, A. 2004, A&A, 419, 47
Galametz, A., et al. 2009, ApJ, 694, 1309
Gehrels, N. 1986, ApJ, 303, 336
Gilmour, R., Best, P., & Almaini, O. 2009, MNRAS, 392, 1509
González, J. J., Krongold, Y., Dultzin, D., Hernández-Toledo, H. M., Huerta, E. M., Olguín, L., Marziani, P., & Cruz-González, I. 2008, RevMexAA Conf. Ser., 32, 170
Johnson, O., Best, P. N., & Almaini, O. 2003, MNRAS, 343, 924
Kim, M., et al. 2007, ApJ, 659, 29
King, I. 1962, AJ, 67, 471
Koulouridis, E., Plionis, M., Chavushyan, V., Dultzin, D., Krongold, Y., Georgantopoulos, I., & Goudis, C. 2009, arXiv:0910.1355
Koulouridis, E., Plionis, M., Chavushyan, V., Dultzin-Hacyan, D., Krongold, Y., & Goudis, C. 2006, ApJ, 639, 37
Lee, J. H., Lee, M. G., Park, C., & Choi, Y.-Y. 2010, MNRAS, 401, 1804
Martini, P., Kelson, D. D., Mulchaey, J. S., & Trager, S. C. 2002, ApJ, 576, L109
Martini, P., Mulchaey, J. S., & Kelson, D. D. 2007, ApJ, 664, 761
Martini, P., Sivakoff, G. R., & Mulchaey, J. S. 2009, ApJ, 701, 66
Molnar, S. M., Hughes, J. P., Donahue, M., & Joy, M. 2002, ApJ, 573, L91
Padilla, N., Lambas, D. G., & González, R. 2009, arXiv:0911.5345
Poggianti, B. M. 1997, A&AS, 122, 399
Ruderman, J. T., & Ebeling, H. 2005, ApJ, 623, L81
Schlegel, D. J., Finkbeiner, D. P., & Davis, M. 1998, ApJ, 500, 525
Shen, Y., Mulchaey, J. S., Raychaudhury, S., Rasmussen, J., & Ponman, T. J. 2007, ApJ, 654, L115
Silverman, J., et al. 2009, ApJ, 695, 171
Sorrentino, G., Radovich, M., & Rifatto, A. 2006, A&A, 451, 809
van Breukelen, C., et al. 2009, MNRAS, 395, 11
von der Linden, A., Wild, V., Kauffmann, G., White, S. D. M., & Weinmann, S. 2009, arXiv:0909.3522